Predictive versus Classic Control of the Induction Motor Drives

Sergiu Ivanov[1], Vladimir Răsvan[2], Eugen Bobaşu[2], Dan Popescu[2], Florin Stîngă[2], Virginia Ivanov[1]
[1] University of Craiova, Faculty of Electrical Engineering, Romania, sergiu.ivanov@ie.ucv.ro, vivanov@elth.ucv.ro
[2] University of Craiova, Faculty of Automation, Computer and Electronics,
[vrasvan, ebobasu, dpopescu, florin]@automation.ucv.ro

***Abstract* - The paper deals with techniques which use the predictive concepts in order to obtain both the pulse width modulation strategy of a voltage fed inverter and the predictive control of the induction motor drive. Concerning the PWM technique, it is applied for the case when the inverter supplies an induction motor, the reference values of the currents being obtained from a classical vector control scheme. The described technique is then simulated and the waveforms are compared with ones obtained with preset currents (bang-bang) pulse width modulation, as the behavior of the two strategies is similar. The results are also compared with the ones resulted when a classical DTC controls the induction motor, as the both determine, during each sampling period, the next stator voltage phasor, but considering different criteria. Concerning the control of the drive, the vector control and the predictive control of the induction motor are compared. For the vector control, the rotor flux oriented one is pointed out, with highlight on the voltage source inverter type. A simple (and practical) method for avoiding the influences of the stator resistance variations when a voltage source inverter is used is presented, based on proper simulation models. For the predictive control of the induction motor, a sensorless diagram is considered. Finally, further actions are proposed for the work continuation.**

Keywords: *voltage inverter, induction motor, vector control, predictive control.*

I. INTRODUCTION

Nowadays, the hardware topologies of the inverters designed to supply the induction motors in variable speed drives are well crystallized. Besides quite special architectures, basically, there are the two level inverter (the classical three phase, six switches, bridge) and the multilevel inverters designed for very high power or voltage applications [1, 2].

Concerning control techniques of the inverters, the strategies are practically unlimited, the literature being quite rich and dynamic [3-5]. Even the classification of these strategies can be performed by considering different criterions. We will take into account here only the source type which the inverter has: voltage or current. We consider only the inverters which are supplied by a DC link having voltage source behavior.

We must see the modulation strategy only as a vector for obtaining the control of the whole driving system, which finally means the control of the developed torque.

Even from the basics of the vector stated by Leonhard, Blaschke and their followers in the 1970s, in rotating references, oriented after the rotor flux, stator flux or magnetizing flux respectively, there is an obvious decoupling between the two components of the stator current: while the direct component acts on the flux modulus only and produces the reactive component, the quadrature component generates the torque, being the active component. The two components of the stator current must be thus controlled independently and the flux and torque generation are thus decoupled, similarly to the DC motor.

Due to results simplicity, the rotor flux oriented control has imposed almost as a standard. From here there were engineered direct control drives (where flux position and modulus are known while the reactive and active components of the stator current are computed in the proper reference frame using the set-point torque and flux) and indirect control drives (where the slip frequency is computed and imposed without direct knowledge of the flux while the reference system change from the flux-reference to stator-reference one is performed by integration of the sum of the motor speed and the speed corresponding to the computed slip.

This means that, as the torque is controlled by the current components, a current source inverter is more suited for the control of the torque developed by the drive. The previous work of the authors emphasized that the field oriented control (FOC) schemes based on current source inverters (preset currents, or bang-bang modulation) are more robust to the parameters variations and have very good dynamics. The main disadvantages of this simple modulation strategy are related to the necessary very high switching frequency (available only in the low range of power), variable switching frequency (difficult to estimate the losses) and interphases dependency. Different techniques were developed for improving the strategy (sinusoidal hysterezis, multilevel hysteresis comparators [6], but the variable switching frequency rests always as a disadvantage.

The technique we propose has the behavior of preset currents inverter, but it performs the pulse width modulation with fixed frequency, which is in fact the sampling frequency of the system.

From this point of view (fixed switching frequency given by the sampling one), the proposed technique has a similarity with another very simple method for the toque control, the Direct Torque Control (DTC), suited for electrical traction applications [7-13]. As will be shown, as the direct controlled variables are the stator currents, the behavior of the proposed technique is much better.

The predictive control has established itself in the last 5-7 years as a very proficient form of controlling highly nonlinear and uncertain systems; moreover the most recent results show its applicability to fast processes among which drives and their converters have a central position [14-17].

The paper will briefly present the basics of the vector control for the rotor flux oriented control for voltage source inverter, with highlight on the influence of the parameters variations on the drive performance. A simple method for reducing these influences will be discussed based on appropriated models. Then a presentation of the predictive control applied to the induction motor will be considered, based on a Simulink model. Finally, conclusions will be issued and ideas for continuation will be pointed out.

II. Basics of Predictive Control

The model predictive control is a control technique which has been successfully implemented in industry. The predictive control techniques were used to control both continuous as well as discrete systems [20-24].

The predictive control is derived from optimal control, yet, in this case the optimal control problem involves additional constraints.

The predictive control techniques require solving an open loop optimal control problem, taking into account constraints on input, state and/or output variables. At every moment *k*, the measured variables and the model of the process are used to compute (to predict) the future behavior of the system over a prediction horizon *N* (Fig. 1).

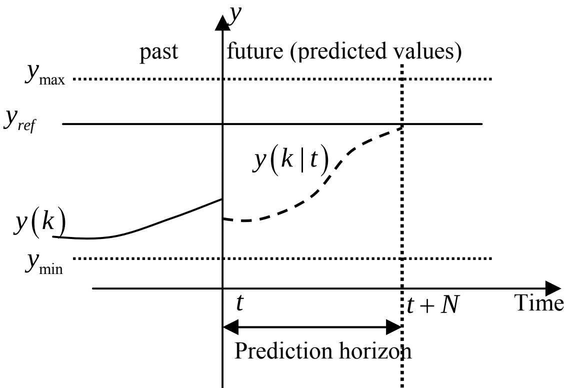

Fig. 1. Evolution of system output using predictive control strategy.

This task is accomplished by determining a set of future control inputs such that the objectives and the system constraints are satisfied. The control input is determined by minimization of a cost function over a time horizon N_c.

Generally, the cost function used in predictive control is defined as follows:

$$J(k)=\sum_{t=1}^{N}\left\|y(k|t)-y_{ref}(k)\right\|^{2}_{Q(t)}+\sum_{t=1}^{N_c}\left\|u(k|t)\right\|^{2}_{R(t)} \qquad (1)$$

subject to constraints specified on the inputs, outputs and input increments (Fig. 2):

$$u_{min}\le u(k)\le u_{max}\ ,$$

$$y_{min}\le y(k)\le y_{max}\ ,$$

where:

$Q(t)$ - positive definite error weighting matrix;

$R(t)$ - positive semi-definite control weighting matrix;

$y(k|t)$ - vector of predicted output signals;

$y_{ref}(k)$ - vector of future set points;

$u(k|t)$ - vector of future control inputs;

N - prediction horizon;

N_c - control horizon.

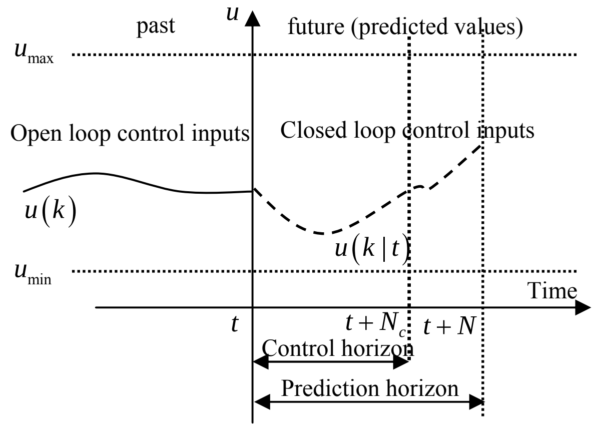

Fig. 2. The control inputs applied to the system using the predictive control strategy.

III. Predictive Control of the Three Phase Inverter

The basic ideas of the predictive control of the three phase bridge inverter are presented in [19] for a simple R-L load.

The predictive command of the inverter is facilitated by the limited number of possible future states. In fact, the inverter can have only eight different topologies (Fig. 3). These eight different topologies determine seven positions of the voltage phasor (Fig. 4). It is to note that two topologies (7 and 8) are equivalent and determine the same position of the voltage phasor. In practice, one of the two is chosen depending on the actual state of the inverter in order to minimize the number of switches. If the actual state is one of 2, 4 or 6 and the zero phasor must be obtained, the topology 7 will be chosen. Contrary, if the actual state is one of 1, 3 or 5 and the zero phasor must be obtained, the topology 8 will be chosen.

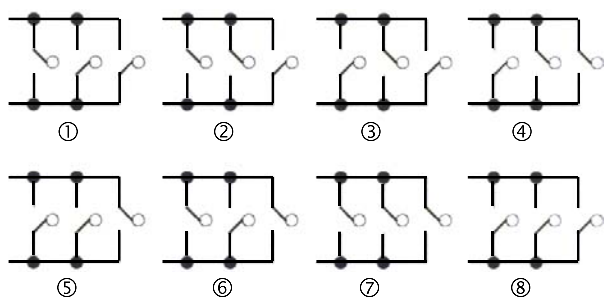

Fig. 3. Possible topologies of the three phase bridge.

The operating principle is to compute at each sampling step the estimations of the (α, β) components of the currents, i^e_α, i^e_β, for all the seven different values of the voltages corresponding to different topologies.

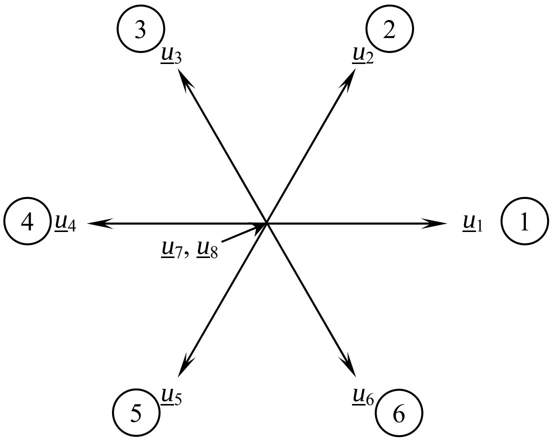

Fig. 4. Positions of the voltage phasor.

Then, the topology that will be applied for the next sampling period will be chosen the one which minimises the cost function

$$J(k)=\left|i_\alpha^*(k+1)-i_\alpha^e(k+1)\right|+\left|i_\beta^*(k+1)-i_\beta^e(k+1)\right|, \qquad (2)$$

where i_α^*, i_β^* are the preset values of the (α, β) components of the currents.

The principle described above will be applied considering as load of the inverter, an induction machine.

At each sampling period, having as initial conditions the actual values of the stator and rotor currents components, $i_{s\alpha}$, $i_{s\beta}$, $i_{r\alpha}$, $i_{r\beta}$, the state equation model of the motor (3) is integrated for all the seven different values of the input vector, which consists in the voltage components $[uu]=\left[u_{s\alpha},\ u_{s\beta},\ u_{r\alpha},\ u_{r\beta}\right]^T$,

$$\frac{d}{dt}[i]=[ML]^{-1}\left([uu]-\left([MR]+[MXr]\right)\cdot[i]\right), \qquad (3)$$

where:

$[i]=\left[i_{s\alpha},\ i_{s\beta},\ i_{r\alpha},\ i_{r\beta}\right]^T$ - the stator and rotor (α, β) current components;

$[ML]=\begin{bmatrix} L_s & 0 & L_m & 0 \\ 0 & L_s & 0 & L_m \\ L_m & 0 & L_r & 0 \\ 0 & L_m & 0 & L_r \end{bmatrix}$ - the inductances matrix, whose components are:

L_s, L_r – total stator and rotor inductances;
L_m – mutual inductance;

$[MR]=\begin{bmatrix} R_s & 0 & 0 & 0 \\ 0 & R_s & 0 & 0 \\ 0 & 0 & R_r & 0 \\ 0 & 0 & 0 & R_r \end{bmatrix}$ - the resistances matrix;

$[MXr]=\begin{bmatrix} 0 & 0 & 0 & 0 \\ 0 & 0 & 0 & 0 \\ 0 & P\omega_r L_m & 0 & P\omega_r L_r \\ -P\omega_r L_m & 0 & -P\omega_r L_r & 0 \end{bmatrix}$ - the reactance matrix, whose terms depend on the

P – number of pairs of poles and
ω_r – mechanical speed of the rotor.

The model (3) is completed with the movement equation which must be also be integrated at each sampling period

$$\frac{d\omega_r}{dt}=\frac{1}{J}\left[\frac{3}{2}PL_m\left(i_{s\beta}i_{r\alpha}-i_{s\alpha}i_{r\beta}\right)-T_s\right], \qquad (4)$$

where:
J – total inertia at the motor shaft;
T_s – static torque applied to the rotor shaft.

It result seven sets of state variables estimations

$$\left[i_{s\alpha}^e,\ i_{s\beta}^e,\ i_{r\alpha}^e,\ i_{r\beta}^e,\ \omega_r^e\right]_{1\cdots7}$$

and the cost function (2) is computed for the stator currents components

$$J(k)\Big|_{1\ldots7}=\left|i_{s\alpha}^*-i_{s\alpha}^e\right|+\left|i_{s\beta}^*-i_{s\beta}^e\right|. \qquad (5)$$

The next topology of the inverter is chosen the one which corresponds to the minimum of the seven values given by (5).

The preset values of the stator currents components $i_{s\alpha}^*, i_{s\beta}^*$ are the results of a classical FOC of the induction machine supplied by a preset currents inverter, Fig.5.

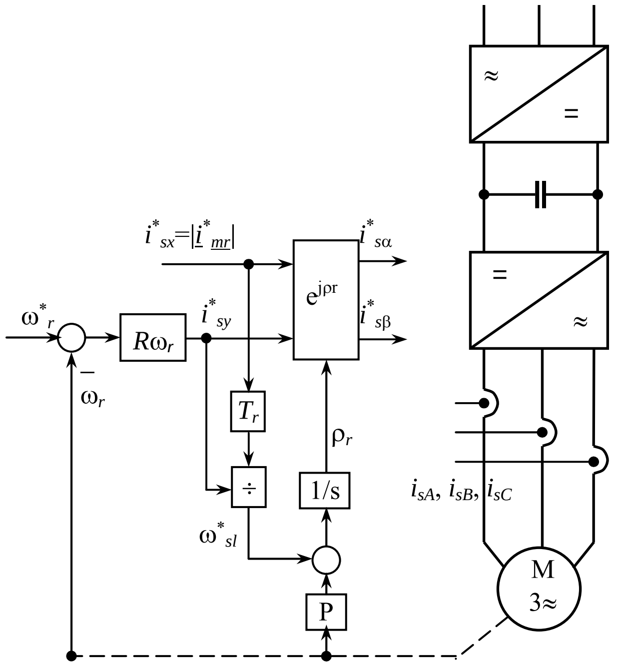

Fig. 5. Stator currents for preset currents modulation.

The block which estimates the currents and computes the cost function (5) must be placed between the rotation transformation block $e^{j\rho r}$ and the inverter.

IV. Simulink Model of the Inverter Control

The complete Simulink model of the inverter control is depicted in Fig. 6.

As can be seen, the classical FOC (upper part of the figure) outputs the preset values of the two stator currents components. They are applied (by the way of GoTo tags) to the Optim switch block. This block (Fig. 7) computes all the currents in the model (3) and the speed (4), for all the seven possible values of the stator voltages (blocks I_1 to I_7).

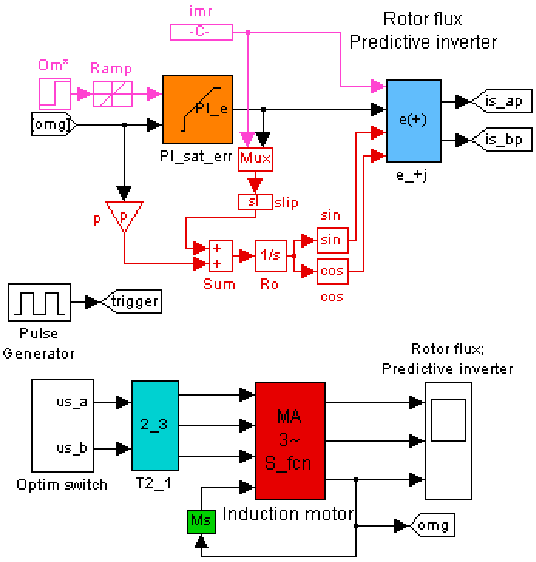

Fig. 6. Simulink model of the inverter control.

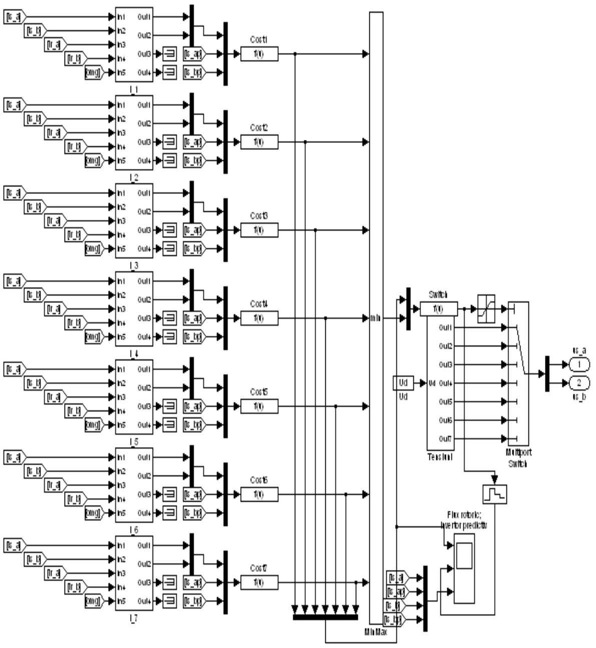

Fig. 7. The optim switch block.

Each of the seven blocks computes the estimated values of the stator and rotor currents components based on (3), the integrators being reset with the actual values of the four currents components (Fig. 8).

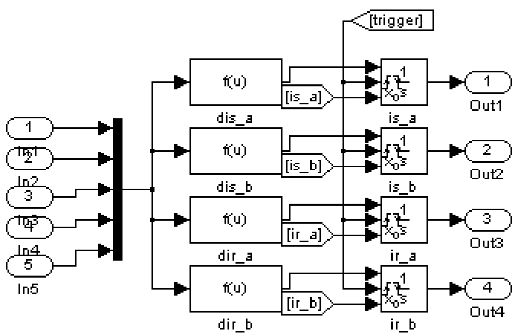

Fig. 8. The computing of the stator and rotor currents components.

The cost function (5) is then computed for all the seven possible values of the stator voltages, then the minimum of the seven is determined and it is identified the topology which determines that this minimum is achieved. The output vector consists of the two stator voltage components, $u_{s\alpha}$, $u_{s\beta}$, the rotor being considered squirrel cage and consequently, $u_{r\alpha} = u_{r\beta} = 0$.

V. SIMULATION RESULTS AND COMPARISONS

The simulation results of three types of command are presented in Fig. 9, 10 and 11, in all cases the simulation step being constant and equal to 100 µs. Only the phase currents are plotted as results of the simulations, the comparison being performed from this point of view. Of course, a better (smaller) ripple of the phase currents determines better overall behaviour of the drive (smaller torque ripple, greater average torque and better dynamics).

Fig. 9 plots a detail of the currents obtained by using the presented technique.

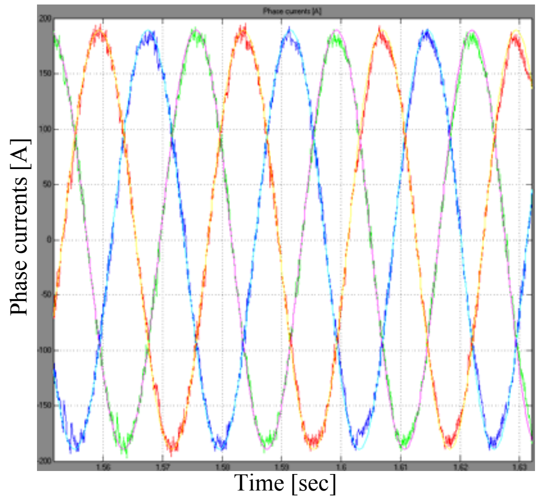

Fig. 9. Stator currents for predictive command of the inverter.

These waveforms must be compared with the ones obtained with a classical bang-bang modulator (preset currents), but with fixed switching frequency (the same as for predictive control). In this case (Fig. 10), the ripple of the currents is significantly higher.

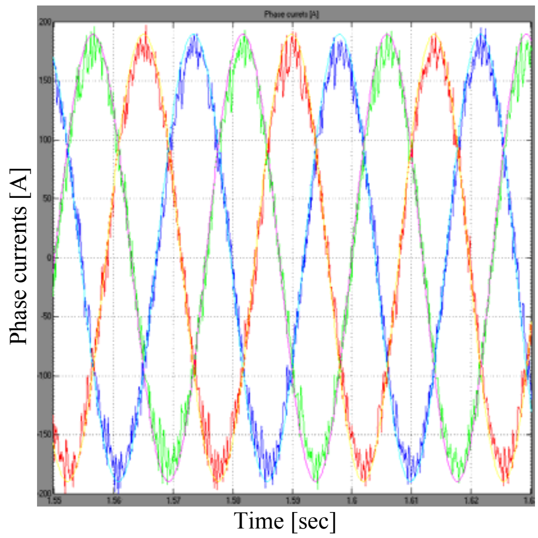

Fig. 10. Stator currents for preset currents modulation.

We notice that, for the same constant switching frequency, the current ripple can arise to be four times larger (40 A, compared with 10A). This is because, for preset currents (bang-bang) modulation, the switches are obtained independently on the three phases. For the predictive modulation, the topology of the inverter is chosen globally, as the one which minimizes the currents errors.

Finally, the waveforms are compared with the ones resulted when a classical DTC controls the induction motor. Once again, the sampling period is the same 100 µs. We make this comparison due to the similarity of the commands: the both determine the next stator voltage phasor, but considering different criteria.

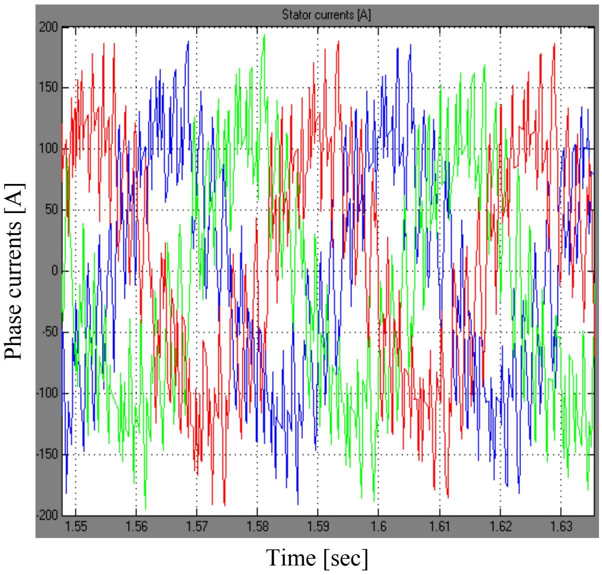

Fig. 11. Stator currents for classical DTC.

We notice that the results are the worst, from the point of view of currents ripple.

All the simulations were performed for a 55 kW motor, 981 min^{-1}.

VI. Vector Control of the Induction Motor

As stated above, the vector control strategy most often used is the rotor flux oriented one. The reasons reside in the simplicity of the expressions resulted from the rotor voltage equation which mainly gives the rotor flux speed and further, by integration, the rotor flux position, used at its turn for the transformation of the reference currents/voltages from the rotary frame to the stationary one.

By identifying the terms on each of the axes d, q, the following two expressions result which are the simplest among all the vector control types

$$T_r \frac{d\left|\underline{i}_{mr}\right|}{dt} + \left|\underline{i}_{mr}\right| = i_{sd}, \tag{6}$$

$$\omega_{mr} = P\omega_r + \frac{i_{sq}}{T_r\left|\underline{i}_{mr}\right|}. \tag{7}$$

We notice from (6) that if the flux is kept constant ($\left|\underline{i}_{mr}\right| = \text{ct.}$), then $\left|\underline{i}_{mr}\right| = i_{sd} = \text{ct.}$ As the electromagnetic torque expressed in the rotor flux oriented frame is

$$t_e = \frac{3}{2} P \frac{L_m^2}{L_r} i_{sd} \cdot i_{sq}, \tag{8}$$

from (7) and (8) results that the slip speed (term 2 in (7)) is proportional with the torque and further, the mechanical characteristic of the induction motor are straight lines, quite similar to the DC motor.

When the motor is supplied by a voltage source inverter, the necessary voltages are obtained by considering the stator voltages equation. By assuming some hypothesis ($\left|\underline{i}_{mr}\right| = i_{sd} = \text{ct.}$, $i_{sq} = \text{ct.}$), it finally result simplified expressions of the preset voltages:

$$u_{sd}^* = R_s i_{sd}^* - \omega_{mr} L_s' i_{sq}^*, \tag{9}$$

$$u_{sq}^* = R_s i_{sq}^* + \omega_{mr} L_s i_{sd}^*, \tag{10}$$

where the second term of each equation will determine the structure of the so called decoupling circuit. The expressions (9) and (10) depend also by the stator resistance. In practice, this dependency induces errors in command. On one hand, by considering only the value of the stator resistance, the “parasitic” voltage drops (on semiconductors, cables, DC circuit in high dynamics) are neglected. The consequences are on the final currents, which do not follow the preset values and consequently, the torque is much smaller than the expected one. Experimentally increasing the value of the resistance used in (9) and (10), the two currents can reach the preset values and the developed torque attains the expected value. But these results are obtained with a value of the equivalent stator resistance which can be double that the stator resistance itself.

This observation raises another question: what happens in practice when the real resistance of the motor changes (increases) during the operation due to the temperature. The expected results could be the same if the decoupling circuit does not adapt itself.

In practice, the decoupling circuit is replaced by two controllers, one for each component of the stator current, Fig. 12.

In addition, the flux speed and position are computed based on the real values of the two components of the stator current. The results of the simulation, plotted in Fig. 13 show a very good behavior, without any transients when the speed reference changes.

This is the type of control industrially implemented, for example in the dsPIC30F from Microchip.

By using in the motor model different values of the stator resistance (alteration due to the temperature for example), the results do not change almost at all. This observation leads to the conclusion that this type of control is much less sensitive to the parameters’ variations.

VII. Predictive Control of the Induction Motor

The model is based on the ideas presented in [19]. The model of the motor is written in the stationary frame (α, β), in terms of stator currents and rotor flux. The outputs chosen to be controlled are the mechanical speed and the modulus of the rotor flux.

The control diagram uses a state observer based on the motor model, adjustable on basis of stator currents errors. It results the sensorless diagram depicted in Fig. 14.

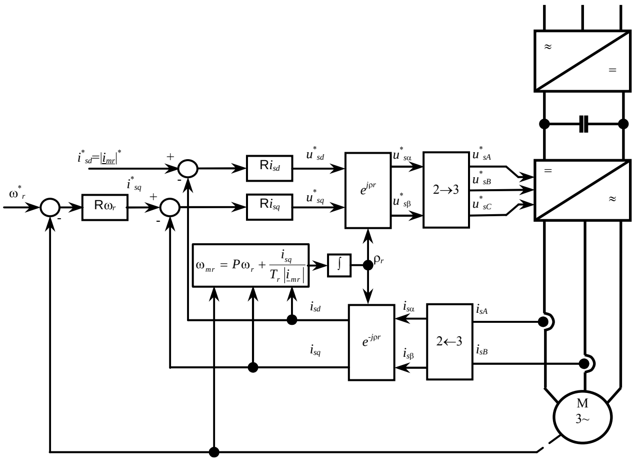

Fig. 12. Decoupling circuit replaced by current controllers.

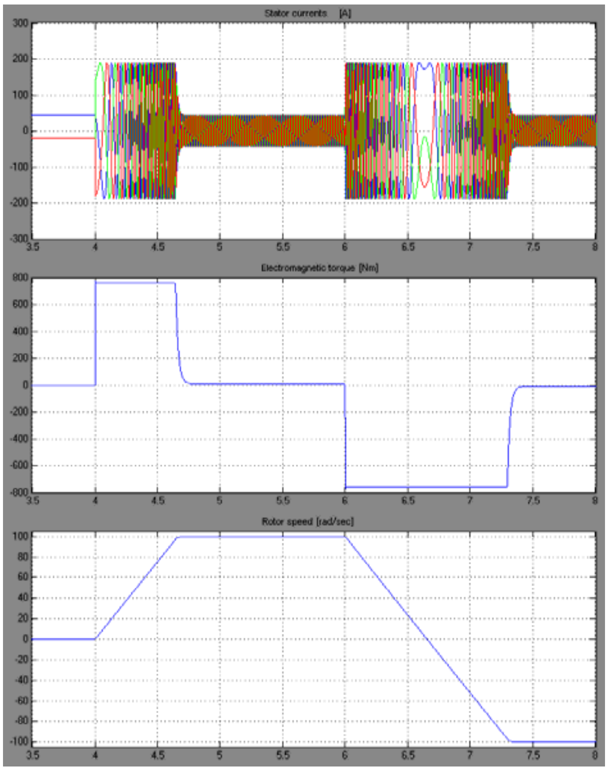

Fig. 13. Simulation of the rotor flux oriented control with current controllers.

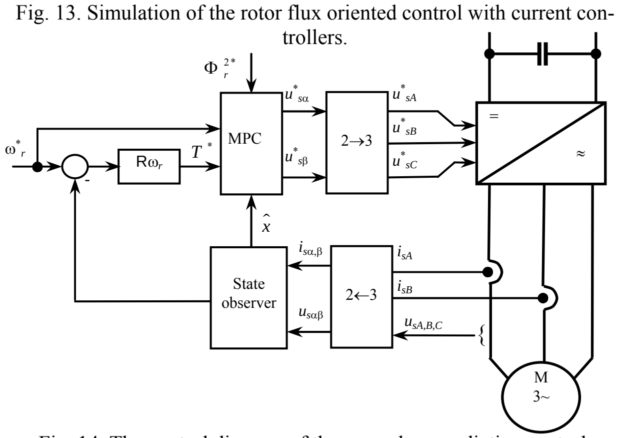

Fig. 14. The control diagram of the sensorless predictive control.

The simulation of the control system for the same operation as in Fig. 13 determined the evolutions plotted in Fig. 15. This time, the currents plot displays the (α, β) components.

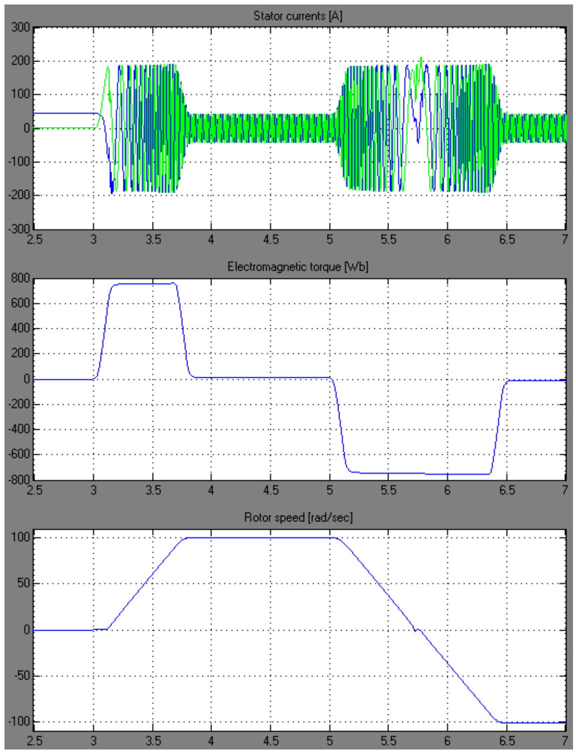

Fig. 15. Simulation of the sensorless predictive control of the induction motor.

It is noticed that the general behaviour of the drive keeps good shapes for the plotted signals.

For comparison with other sensorless controls (flux observer, extended Gopinath observer) [25, 26], the response is comparable, but with less computing effort.

VIII. CONCLUSIONS

The paper describes a strategy for pulse width modulation of the inverters which supply induction machines, based on the predictive technique and a model predictive control of the induction motor.

Concerning the PWM strategy, the results of the simulation are compared, for similar conditions (same fixed step), with another well known modulation technique, preset currents (bang-bang) and classic DTC. The currents ripple is smaller when the proposed modulation technique is used. The consequences are favorable in what concerns the torque ripple and the general dynamic behavior.

In what concerns the control of the drive, the results plotted in Fig. 15, compared with the classic FOC in Fig. 13, show that the dynamic performances are slightly reduced (acceleration time 0.8 seconds), but the advantages of the sensorless control must be underlined, suited for applications like the one described in [27].

ACKNOWLEDGMENT

Authors whish to thank the UEFISCDI and their partners in the HYDICO project (PN-II-PT-PCCA-2011-3.2-1082), in the frame of which their study has been performed.

Received on July 4, 2015
Editorial Approval on November 18, 2015

REFERENCES

[1] D. Moller, C. Schlegel, “Further Development of the ICE for Worldwide Use”, *Elektrische Bahnen* 104, Nr. 5, 2006, pp. 258-263.

[2] A. Steimel, “Power-Electronics Issues of Modern Electric Railway Systems”, in *Advances in Electrical and Computer Engineering*, vol. 10, no. 2, 2010, pp. 3-10, doi:10.4316/AECE.2010.02001.

[3] K. Hartani, Y. Miloud, “Control Strategy for Three Phase Voltage Source PWM Rectifier Based on the Space Vector Modulation”, in *Advances in Electrical and Computer Engineering*, vol. 10, no. 3, 2010, pp. 61-65, doi:10.4316/AECE.2010.03010.

[4] O. Ursaru, C. Aghion, M. Lucanu, L. Tigaeru, “Pulse width Modulation Command Systems Used for the Optimization of Three Phase Inverters”, in *Advances in Electrical and Computer Engineering*, vol. 9, no. 1, 2009, pp. 22-27, doi:10.4316/AECE.2009.01004.

[5] D. Milicevic, V. Katic, Z. Corba, M. Greconici, “New Space Vector Selection Scheme for VSI Supplied Dual Three-Phase Induction Machine”, in *Advances in Electrical and Computer Engineering*, vol. 13, no. 1, 2013, pp. 59-64, doi:10.4316/AECE.2013.01010.

[6] M. Mohseni, S.M Islam, “A New Vector-Based Hysteresis Current Control Scheme for Three-Phase PWM Voltage-Source Inverters”, in *IEEE Transactions on Power Electronics*, Volume 25, Issue: 9, Sept. 2010, 2299 – 2309.

[7] I. Takahashi, T. Noguchi T. 1986. “A new quick-response and high efficiency control strategy of an induction motor”, in *IEEE Transactions on Industrial Applications*. vol. IA-22, no.5, pp. 820-827, 1986.

[8] U. Baader et al, “Direct self control (DSC) of inverter-fed induction machine: a basis for speed control without speed measurement”, in *IEEE Transactions on Industrial Applications*, vol. 28, pp. 581–588, 1992.

[9] M. Ehsani et al, “Propulsion system design of electric and hybrid vehicles”, in *IEEE Trans. Industrial Electronics*, vol. 45, nr.1, pp 19-27, 1997.

[10] J. Faiz et al., “Direct torque control of induction motor for electric propulsion systems”, in *International Journal on Power Systems*, vol. 51, pp. 95–101, 1999.

[11] A. Haddoun et al, “A loss-minimization DTC Scheme for EV Induction Motor”, in *IEEE Transactions on vehicle technology*, vol.56, nr.1, pp.81-88, 2007.

[12] S. Ivanov, “The influence of the sampling period on the performance of the regulation by DTC of the induction motor”, in *Proceedings of the 23rd European Conference on Modelling and Simulation*, Madrid, Spain, 776-780, 2009.

[13] S. Ivanov, “Continuous DTC of the Induction Motor”, in *Advances in Electrical and Computer Engineering*, vol. 10, no. 4, 149-154, 2010.

[14] S. Seo et al., “Hybrid Control System for Managing Voltage and Reactive Power”, in *JEJU Power System, Journal of Electrical Eng. and Technol*. Vol. 4, no.4, 2009, pp. 429-437.

[15] C. Prieur, S. Tarbouriech., “New directions in hybrid control systems” (editorial), in *Int. Journal Robust Nonlin. Control,* Vol. 21, 2011, pp. 1063-1065.

[16] T. Geyer et al., “Hybrid Model Predictive Control of the Step Down DC-DC Converter”, in *IEEE Trans. Contr. Syst. Technol,* Vol. 16, no.6, 2008, pp. 1112-1124.

[17] T. Geyer T., “Model Predictive Direct Torque Control—Part I: Concept, Algorithm, and Analysis”, in *IEEE Transactions on Industrial Electronics*, Vol. 56, no.6, 2009, pp. 1894-1905.

[18] J. Rodriguez, P. Cortes, *Predictive Control of Power Converters and Electrical Drives*, Wiley, 2012.

[19] A. Merabet, *Nonlinear model predictive control for induction motor drive* – chapter in *Frontiers of Model Predictive Control*, edited by Zheng, T, Intechweb.org, 2012, pp. 109-130.

[20] E.F. Camacho, C. Bordons, *Model predictive control*. Springer-Verlag, 2004.

[21] A. Bemporad. *Model predictive control of hybrid systems*, 2nd HYCON PhD. School on Hybrid Systems, Siena, 2007.

[22] M. Lazăr M, *Model Predictive Control of Hybrid Systems: Stability and Robustness*, Ph.D. Thesis, Eindhoven, Holland, 2006.

[23] J.M. Maciejowski, *Predictive control with constraints*, Prentince Hall, 2000.

[24] F. Stinga, *Control strategies for hybrid systems. Applications*, Ph.D. Thesis, Craiova, Romania, 2012.

[25] O. Stoicuţă, T. Pană, “Speed and rotor flux observer for sensorless induction motor drives”, in 2012 *IEEE International Conference on Automation, Quality and Testing, Robotics*, AQTR 2012 - Proceedings, pp. 68-73, 2012.

[26] T. Pană, O. Stoicuţă, “Small Speed Asymptotic Stability Study of an Induction Motor Sensorless Speed Control System with Extended Gopinath Observer”, in *Advances in Electrical and Computer Engineering*, vol. 11, no. 2, pp. 15-22, 2011.

[27] M. Ciontu, D. Popescu, M. Motocu, “Analysis of Energy Efficiency by Replacing the Throttle Valve with Variable Speed Drive Condensate Pump from E.C. Turceni”, in 3rd International Symposium on Electrical and Electronics Engineering (ISEEE), 2010, ISBN 978-1-4244-8407-2, NSPEC Accession Number:11651342, DOI:10.1109/ISEEE.2010.5628495